第 48 卷 第 8 期/2021 年 4 月/中国激光 研究论文

中国激光

基于飞秒激光还原氧化石墨烯的 SiC 纳米线接头电学增强

霍金鹏[1]，肖宇[1]，孙天鸣[1,2]，邢松龄[1]，沈道智[1]，林路禅[1,3]，刘磊[1*]

[1]清华大学机械工程系摩擦学国家重点实验室，北京 100084；

[2]太原理工大学材料科学与工程学院，山西 太原 030024；

[3]瑞士联邦材料科学与技术研究所，瑞士 苏黎世

摘要 纳米线连接为高性能微纳器件的组装和应用提供了技术手段，但现有的连接方式对于能量输入的空间精度和外部环境要求较高，其工艺窗口较窄。为改善这一问题，以氧化石墨烯(GO)作为中间连接层的纳米线连接方式，通过干法转移制备了碳化硅(SiC)纳米线-氧化石墨烯(GO)薄膜-SiC 纳米线的结构，并通过飞秒激光辐照还原氧化石墨烯，降低了 SiC 和 GO 之间的势垒，通过层内导电与层间导电的方式形成了更宽的载流子通道，从而显著提升了电流水平。此外生成的还原氧化石墨烯(rGO)纳米膜对 SiC 纳米线的接头形成了包裹与保护作用，从而使接头部分具有更好的抗辐照和热传导性能，提升了器件的稳定性与使用寿命。最后，利用飞秒激光还原 GO 薄膜实现了 SiC 纳米线网络的电性能提升，制备了具有良好响应度和较快响应速度的紫外光传感器及透明柔性导电薄膜等器件。

关键词 激光制造；飞秒激光；碳化硅纳米线；氧化石墨烯；微纳器件

中图分类号 TB383 **文献标志码** A **doi**：10.3788/CJL202148.0802007

1 引 言

随着信息技术、航天技术、生物技术等领域的迅速发展，对于其设备的小型化、集成化、低功耗化与适用场合多元化提出了更高的要求。纳米材料由于其独特的小尺寸效应、表面效应与量子尺寸效应，在新一代半导体器件中具有非常广阔的应用前景[1]。目前，纳米器件与微纳系统封装已经成为了衡量国家电子信息产品核心竞争力的关键指标之一。纳米材料可以用于制备各种高性能、跨尺度器件，例如透明导体电极[2-3]、有机发光二极管(OLED)[4]、传感器[5-6]、热电材料和薄膜太阳能电池[7-8]等。然而，由于未来纳米器件对多材料、跨尺度与广适性的要求越来越高，纳米材料的成形与器件的制备面临着越来越多的挑战。

作为一种自下而上的纳米材料的成形方法，纳米线连接可以将不同的材料性能进行结合，并实现更复杂的器件，如忆阻器[9]、场效应管[10]和跨尺度传感器[11]等。虽然纳米线连接的概念很早被提出，但由于其连接的理论还未完全建立，连接工艺处于初步阶段，纳米线连接仍处于材料成形中的前沿领域。现有的纳米线连接方式主要是利用纳米线的表面效应，与宏观材料相比，纳米线具有较低的熔点，故在较低的力/热源输入方式下会形成原子层相互扩散，从而形成冶金接头。例如对于部分金属纳米材料，可以通过热退火使得接头形成融化区，从而实现纳米线互联，构造纳米线网络[12]；另外，Chen 等[13]通过超声辅助方法实现了碳纳米管和金属电极之间的互联；对于高熔点陶瓷纳米材料，使用电子束或者离子束进行同样的加工可以形成有效的连接[14]。然而，以上方式中传统的力/热输入由于能量输入不具有空间选择性，有可能造成连接结构的

收稿日期：2020-12-01；**修回日期**：2021-01-23；**录用日期**：2021-02-23

基金项目：国家重点研发计划(2017YFB1104900)、国家自然科学基金(51775299，52075287，51520105007)

* **E-mail**：liulei@tsinghua.edu.cn

过度损伤，而高精度的电子束或离子束连接方式又对定位精度与环境条件提出了极高的要求，增加了纳米材料互联的成本与复杂度。

超快激光作为一种直接能量输入的方式，可以通过光学透镜和光电快门较为快捷地对能量输入进行空间和时域调控。此外，纳米尺度下的光辐照还会引起材料的局域表面等离激元效应，从而实现激光能量的空间限制性输入，进一步提高连接中能量输入的空间精度[15-16]。同时，飞秒激光作为一种超快激光，具有脉冲时间短、峰值功率高、热影响区小等优势[17]，可以实现更高熔点纳米材料的连接，例如 Lin 等[18]使用飞秒激光实现了银-二氧化钛纳米线异质结的连接；Xing 等[19]使用飞秒激光，利用多光子吸收效应实现了高熔点氧化锌纳米线之间的互连。

本文通过借鉴传统焊接中的钎焊思路，空间定点引入氧化石墨烯作为辅助导电通路，利用飞秒激光的还原作用与局域能量输入的特点，对氧化石墨烯进行局域还原，并将理论上的点接触接头优化为线接触与面接触，从而提升了 SiC 纳米线接头的电流水平与性能稳定性。此外，进一步研究了还原氧化石墨烯（rGO）纳米薄膜对于结构的保护作用，制备了一系列纳米线网络紫外光（UV）探测器与柔性透明导电薄膜等器件。

2 实验方法

2.1 实验材料

实验用的固态 SiC 纳米线与氧化石墨烯乙醇溶液购于南京先丰纳米公司，将 SiC 纳米线溶入工业乙醇（质量分数≥99.7%）中，超声后制备 SiC 纳米线悬浮液。电学测量所用的 200 nm 厚的叉指电极是采用光刻法沉积在单晶硅基底上，经氧化、光刻、显影、磁控溅射、划片等微电子工艺后制备而成。

2.2 干法转移制备 SiC 纳米线-GO 薄膜-SiC 纳米线结构

采用干法转移制备了 SiC 纳米线-GO 薄膜-SiC 纳米线结构，如图 1(a)所示。单个纳米材料的转移流程是首先用移液枪取 10 μL 的 SiC 纳米线悬浮液和 GO 薄膜悬浮液分别置于聚二甲基硅氧烷（PDMS）上，待乙醇蒸发后利用纳米转移平台在光镜下将 SiC 纳米线移动到指定的位置，与芯片贴合后在 80 ℃条件下保温一段时间即可脱落，SiC 纳米线需保温 10 min，GO 纳米膜需保温 20 min。重复以上步骤即可获得 SiC 纳米线-GO 薄膜-SiC 纳米线结构。

2.3 飞秒激光还原氧化石墨烯

使用功率为 4 W、波长为 800 nm、脉冲宽度为 50 fs、重复频率为 1 kHz 的钛宝石飞秒激光器作为光源辐照 SiC 纳米线接头部位，如图 1(b)所示，经过机械快门、衰减镜、半波片、偏振片后进入光学显微镜，再通过物镜进行聚焦加工，其中机械快门可以控制激光辐照时间，衰减片与偏振片可以控制激光功率密度，电控位移平台可以控制光斑大小，CCD 相机可以实现可视化操作。

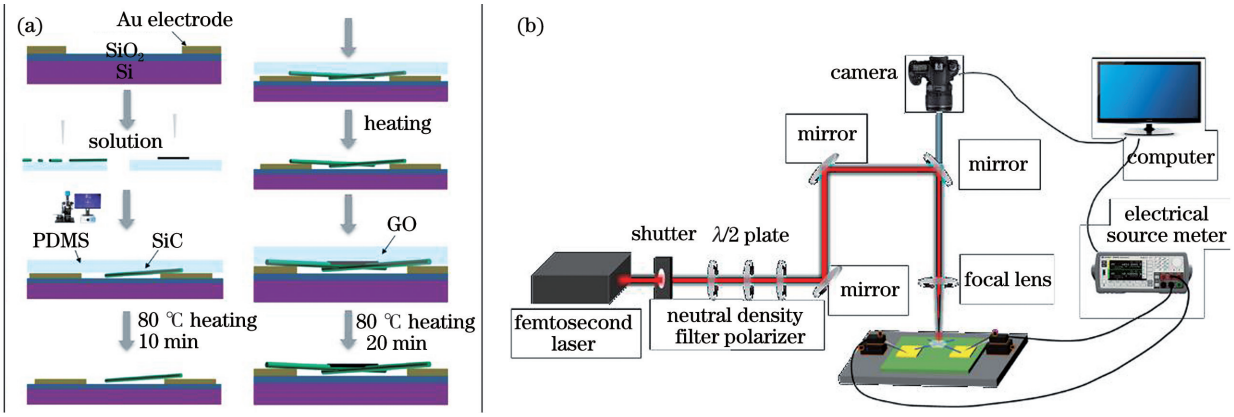

图 1 构建 SiC 纳米线-GO 薄膜-SiC 纳米线结构与飞秒激光辅助连接示意图。(a)干法转移制备 SiC 纳米线-GO 薄膜-SiC 纳米线结构；(b)飞秒激光辐照还原 GO 纳米薄膜与电学测试的示意图

Fig. 1 Schematic diagrams of SiC nanowire-GO film-SiC nanowire structure and femtosecond laser assisted connection. (a) Structure of SiC nanowire-GO film-SiC nanowire was prepared by dry transfer method; (b) schematic diagram of GO nano film reduction by femtosecond laser irradiation

2.4 材料学表征、电学表征与多物理场模拟

采用光学显微镜（Olympus，BX51M）、扫描电镜（SEM，Zeiss Supra 55）和透射显微镜（TEM，JEM-2100F）进行形貌与晶向表征，采用 X 射线衍

射仪(XRD，Bruker D8)对纳米线进行物相分析。采用双源半导体电学测试仪(Keithley 2636B)进行 SiC 纳米线-GO 薄膜-SiC 纳米线结构的电学性能测量。光场辐照模拟采用多物理场有限元模拟软件(COMSOL Multiphysics 5.4)，基于波动光学的频域模块进行建模，光场设置中采用平面波入射，波长为 800 nm，初始入射电场强度设为 1，各对应边界条件为散射边界，材料参数经由手册和相关文献查询[19-20]。

3　实验结果与分析讨论

3.1　SiC 纳米线-GO 薄膜-SiC 纳米线结构的构建与材料学表征

图 2 对 SiC 纳米-GO 薄膜线-SiC 纳米线结构的形貌与电学数据进行了表征。利用干法转移的方式将 SiC 纳米线与氧化石墨烯转移至金电极上，如图 2(a)所示。在光学显微镜下，可以观察到氧化石墨烯为半透明结构，故可以清晰地判断出 SiC 纳米线接头的空间位置，并可利用显微镜平台进行定位。SiC 纳米线的 X 射线衍射(XRD)图像的结果表明，在 35.7°、41.5°、60.1°和 71.9°处出现 4 个尖峰，分别对应于 3C-SiC 的(111)、(200)、(220)、(311)晶面，如图 1(e)所示。图 1(c)、(d)表征了制备的 SiC 纳米线网络与 GO 纳米膜组合的透射电镜(TEM)图像，SiC 的衍射图谱与高分辨图像表明，SiC 纳米线是沿(111)晶向生长的单晶。激光处理过后 SiC 纳米线-SiC 纳米线-氧化石墨烯的结构在扫描电镜(SEM)下的图像如图 2(b)所示，可以看出在激光功率超过 GO 的损伤阈值时 GO 表面会出现一定程度的表面损伤，而 SiC 纳米线的损伤阈值相对于 GO 较高且并未发生明显损伤。图 2(g)表征了层数较少的氧化石墨烯与 SiC 纳米线接触时的 SEM 形貌，可以看出柔性的 GO 纳米薄膜对于 SiC 纳米线形成了包裹作用，从而增大了两种纳米材料之间的接触面积，增强了激光还原后 rGO 与 SiC 纳米线之间的电流导通能力与力学稳定性。

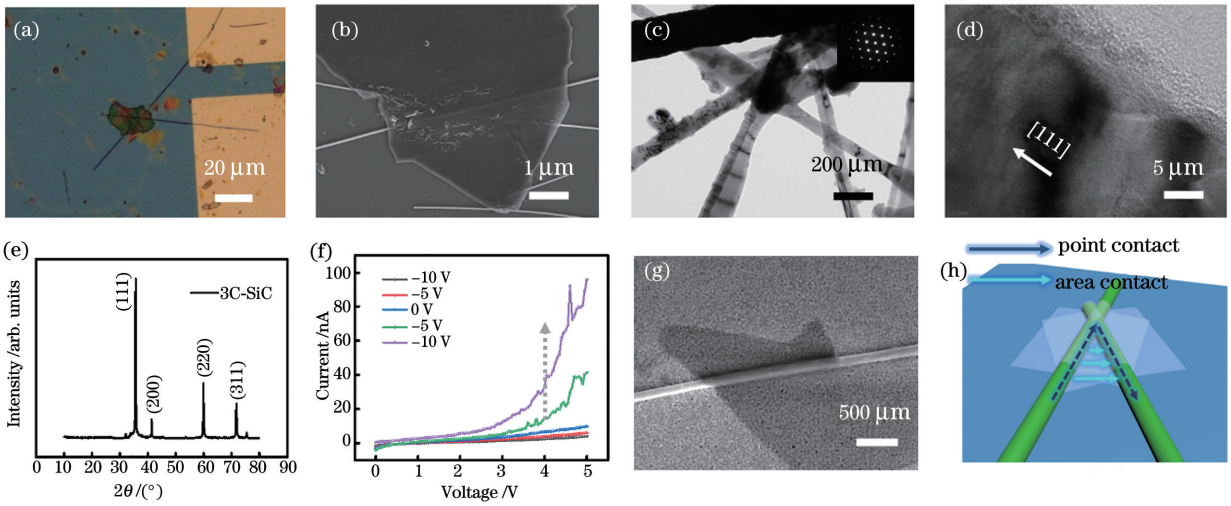

图 2　SiC 纳米线-GO 薄膜-SiC 纳米线结构的形貌与电学数据表征。(a)光学显微镜下被 GO 半透明薄膜覆盖的 SiC 纳米线-SiC 纳米线结构；(b)SiC 纳米线-GO 薄膜-SiC 纳米线的 SEM 图像；(c)SiC 纳米线与 GO 薄膜组成的纳米线网络的 TEM 图像；(d)SiC 纳米线的 TEM 高分辨图像；(e)SiC 纳米线的 XRD 图像；(f)n 型 SiC 纳米线场效应管的背栅特性；(g)少层 GO 薄膜与 SiC 纳米线形成包覆的 SEM 图像；(h)SiC 纳米线-GO 薄膜-SiC 纳米线结构电流通路示意图

Fig. 2　Chemical and electrical characterization of SiC nanowire-GO film-SiC nanowire structure. (a) Structure of SiC nanowire-SiC nanowire covered by GO translucent film under optical microscope; (b) SEM image of SiC nanowire-GO film-SiC nanowire; (c) TEM image of nanowire network composed of SiC nanowire and GO film; (d) high resolution TEM image of SiC nanowires; (e) XRD image of SiC nanowires; (f) electrical characterization of n-type SiC nanowire; (g) SEM image of the coating formed by the few layer GO film and SiC nanowire; (h) schematic diagram of the current path of SiC nanowire-GO film-SiC nanowire structure

3.2　SiC 纳米线-GO-SiC 纳米线结构激光还原效果电学表征

在对于 SiC 纳米线-GO 纳米膜-SiC 纳米线的结构进行材料学表征后，进一步对激光辐照前后的 SiC 纳米线进行电学表征，如图 3 所示。图 3(a)、(b)、(c)分别表示了氧化石墨烯在两根 SiC 纳米线下方、中间和上方的 I-V 曲线。在激光辐照前，图 3(a)和图3(c)的结构在−5～5V的电压下只有

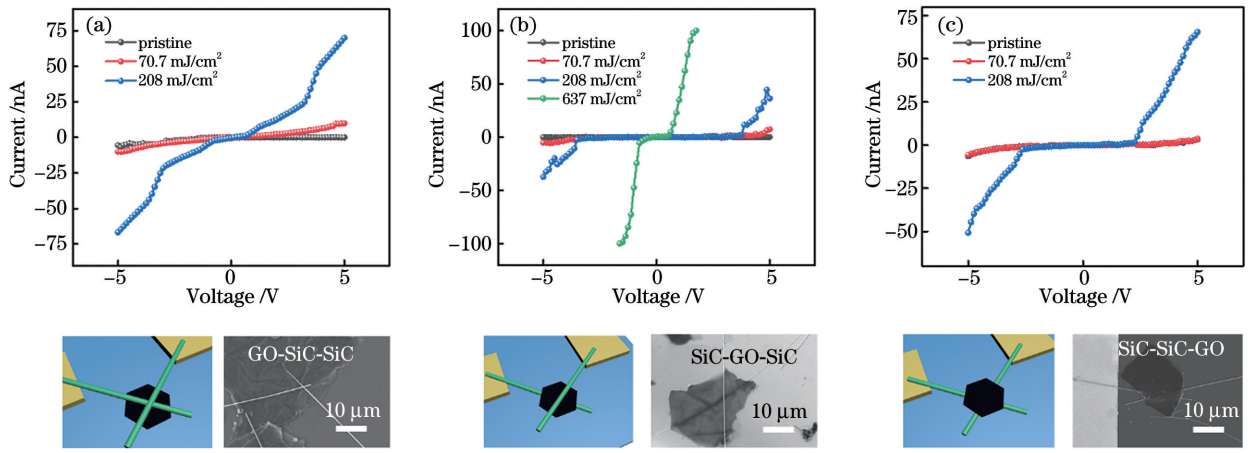

图 3　SiC 纳米线-GO 薄膜-SiC 纳米线结构飞秒激光辐照前后的电学性能表征。(a)GO 薄膜在两根 SiC 纳米线下方；(b)GO 薄膜在两根 SiC 纳米线之间；(c)GO 薄膜在两根 SiC 纳米线上方

Fig. 3　Electrical characterization of SiC nanowire-GO film-SiC nanowire structure before and after femtosecond laser irradiation. (a) GO under two SiC nanowires; (b) GO in the middle of two SiC nanowires; (c) GO above two SiC nanowires

几纳安级别的电流，其原因主要是两根 SiC 纳米线在接头处为点接触，载流子通道过窄导致接头电阻过大，如图 2(h)中的虚线所示；图 3(b)的 SiC 纳米线-GO 薄膜-SiC 纳米线结构在施加两端电压后，电流水平只有皮安级别，其主要原因是绝缘 GO 纳米膜层间电阻极大，阻碍了两根 SiC 纳米线间的载流子流动。

在经过飞秒激光辐照后，3 种复合结构的两端电流水平均有明显的提升，其中：图 3(a)和图 3(c)的结构电学性能提升主要是形成了 SiC 纳米线-rGO 层内-SiC 纳米线的层内导电通路，图 3(b)的结构则是形成了 SiC-rGO 层间与层内的复合导电通路。图 3(b)的结构在飞秒激光还原过后的电流水平最高，其主要原因是该结构中 SiC 纳米线与 GO 薄膜的接触面积最大，形成了更多的载流子通道。

3.3　飞秒激光还原的电学结构导通机理

通过干法转移的方式将氧化石墨烯搭接在金电极的两端，使用不同的飞秒激光功率进行辐照，通过测量其两端的 I-V 曲线可以看出，随着飞秒激光功率密度的升高，GO 经历了先还原后损伤的过程，电导率先升高再降低。在单脉冲能量从 73 mJ/cm² 增加至 247 mJ/cm² 的过程中，GO 表面的含氧基团逐步被还原并使得 GO 的带隙减小，电导率不断升高，峰值相对于初始的 GO 薄膜提升了 6 个数量级，如图 4 所示。在飞秒激光处理过程中，GO 薄膜的颜色会随其还原程度发生变化，利于实验进程中还原程度的实时监测。

在 GO 被超快激光还原后，rGO 与 SiC 之间会

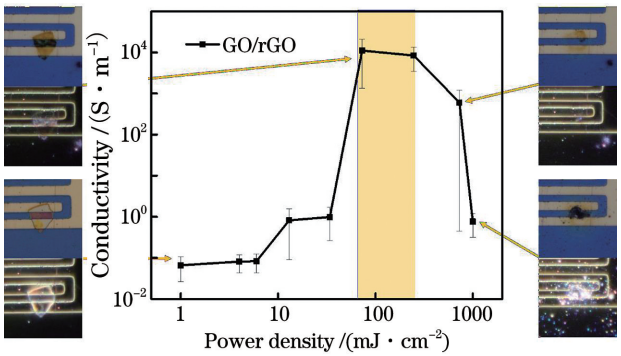

图 4　GO 薄膜在不同功率密度的飞秒激光辐照下的电导率的变化

Fig. 4　Changes of electrical conductivity of GO films irradiated by femtosecond laser with different power densities

形成接触势垒。为了进一步研究 SiC 纳米线与 rGO 费米能级对齐后形成的肖特基接触特性，利用干法转移获得了 GO 纳米膜-SiC 纳米线的异质结，并对于还原前后的电学性能进行了表征，如图 5 所示。对于初始的 GO 纳米膜，其与 SiC 纳米线之间形成的接触势垒较大[21-22]，电流无法导通；在不同功率密度的飞秒激光辐照之后，rGO-SiC 结构的开启电压为 2～5 V，其原因是 GO 纳米膜在激光作用下发生一定程度的还原，从而降低了与 SiC 纳米线之间形成的势垒。由于石墨烯能带的线性色散关系，理论上狄拉克点的态密度为 0，因此激光还原过后形成的 rGO 在和 SiC 半导体接触后，界面载流子的少量输运引起 SiC 和 rGO 的费米能级同时发生移动并达到平衡[23-24]，rGO与SiC的接触势垒相对于

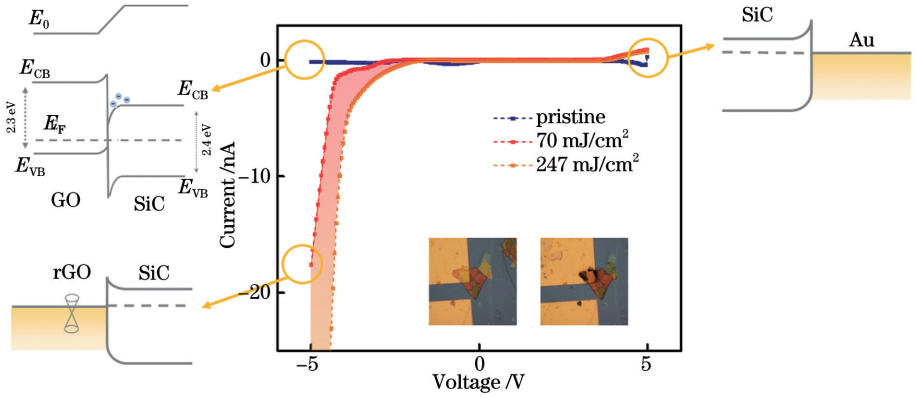

图 5 SiC 纳米线-GO 薄膜在不同功率密度的飞秒激光辐照下的电学响应的变化

Fig. 5 Changes of electrical response of SiC nanowire-GO film irradiated by femtosecond laser at different power densities

Au 有着显著的降低并具有良好的稳定性。相对于其他材料如金属来说，rGO 可以作为一种宽带隙半导体性能良好的纳米连接材料。

上述电学结果表明，氧化石墨烯吸收了飞秒激光的能量并发生了激光-材料的相互作用。本研究进一步通过 COMSOL 模拟软件模拟分析了激光辐照介电环境下 GO 薄膜与 SiC 纳米线之间的能量输入情况。图 6(a)和图 6(b)分别表示了 SiC 纳米线在 GO 上方与下方的情况，空间电场分布表明，曲率变化在石墨烯和纳米线的界面处会产生一定的电场增强，从而进一步促进了 GO 对于飞秒激光的双光子吸收[25-27]，提升了还原效率。同时对 SiC-GO 结构在强场辐照下的结构进行了模拟，结果表明生成的 rGO 对于 SiC 纳米线及其接头会有一定的保护作用，未覆盖 rGO 的一侧，SiC 能量明显增强，如图 6(c)所示；此外，生成的 rGO 具有非常优异的导热性，可以达到 5300 W/(m·K)，利于产生的热量快速扩散。相同功率密度的飞秒激光辐照下，没有被 GO 覆盖的 SiC 纳米线发生了明显的损伤，而被 GO 覆盖的 SiC 纳米线的形貌仍保持完整，如图 6(c)所示。

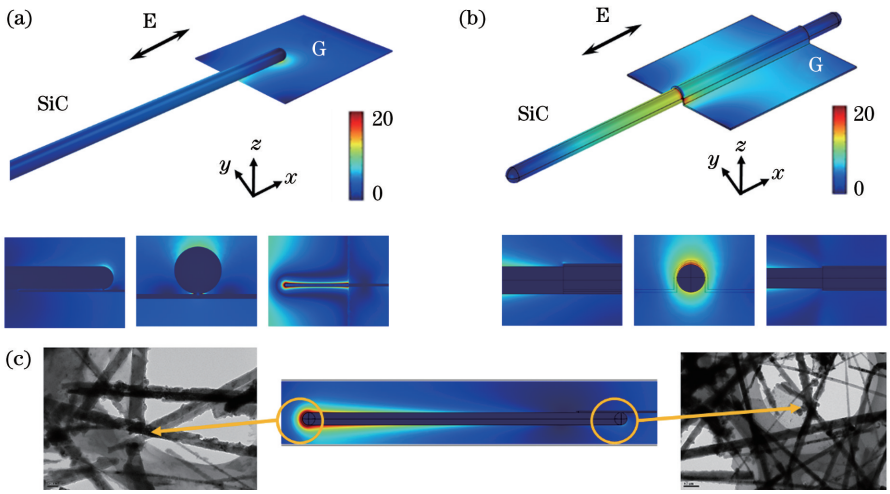

图 6 SiC 纳米线-GO 薄膜结构在激光整体辐照下的电场分布。(a)GO 薄膜在 SiC 纳米线下方时的电场分布；(b)GO 薄膜上方包裹 SiC 纳米线时的电场分布；(c)SiC 纳米线-GO 薄膜结构在大光场下的电场分布

Fig. 6 Field distribution of SiC nanowire-GO film structure under laser irradiation. (a) Field distribution for Go film under SiC nanowire; (b) field distribution for SiC nanowire wrapped by GO film; (c) field distribution for SiC nanowire-GO film structure under the big light field

3.4 基于飞秒激光还原的 SiC 纳米线网络制备与器件性能的改善

飞秒激光辅助还原的 GO 使得 SiC 纳米线之间的电学性能得到了改善，同时由于热影响区小、基体材料未发生相变，基体能够保持半导体的特性，这为进一步制备纳米线网络的跨尺度半导体器件提供了可能性。图 7 表征了使用 SiC 纳米线网络与湿法转移的 GO 纳米膜组成的纳米线导电网络构建的紫外光传感器与柔性透明薄膜。使用能量密度为 636 mJ/cm²，扫描速度为 200 μm/s 的飞秒激光辐

照扫描后，纳米线网络的电流水平从皮安级提升为纳安级。对于 SiC 纳米线网络构建的紫外光传感器件，在受到波长为 375 nm 的紫外光的辐照时，其飞秒激光辐照前后的光电响应特征如图 7(a)所示。初始通过转移平台搭接的 SiC-SiC-GO 网络结构的光传感器在 375 nm 波长下的响应度小于 10^{-5} A/W。在飞秒激光辐照处理后，尽管 SiC 纳米线网络的暗电流有了明显的增加，但相对于焊接之前的纳米线网络，该结构对紫外光表现出良好的响应强度和较快的响应速度，光传感器的响应度约为 0.11 A/W，具有 4 个数量级以上的提升。研究人员一直在积极研究纳米材料，希望开发新型透明导体，特别是柔性导体[28]，本研究利用 SiC 纳米线和 GO 薄膜在 PDMS 上构建了透明的柔性导电薄膜，在进行飞秒激光的扫描辐照后，导电薄膜区域性的电流提升了 5 个数量级以上，如图 7(c)所示，这种柔性透明的导电薄膜在将来可以被应用于可伸展的柔性电极或触摸屏面板上。

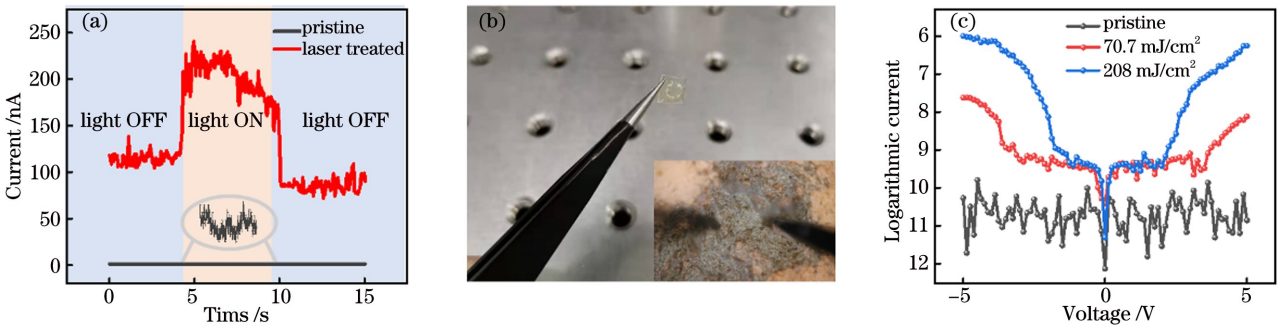

图 7 添加 GO 薄膜的 SiC 纳米线网络的器件应用。(a)SiC 纳米线网络紫外光传感器的光电响应特征；(b)SiC 纳米线网络柔性透明导电薄膜实物图；(c)SiC 纳米线网络柔性透明导电薄膜的电学性能

Fig. 7 Device application of SiC nanowire network with GO films. (a) Photoelectric response characteristics of SiC nanowire network ultraviolet sensors; (b) physical view of SiC nanowire network flexible transparent conductive films; (c) electrical characterization of SiC nanowire network flexible transparent conductive films

4 结 论

通过干法转移制备了 SiC 纳米线-GO 薄膜-SiC 纳米线的结构，在飞秒激光辐照下，氧化石墨烯可以通过双光子吸收作用有效还原，生成具有良好导电性的还原氧化石墨烯。对于不同构型的 SiC 纳米线-GO 薄膜-SiC 纳米线结构，均可以通过飞秒激光还原作用降低 SiC 和 GO 之间势垒，通过层内导电和层间导电的方式形成更宽的载流子通道，从而显著降低阻抗，提升电流水平。生成的 rGO 纳米膜对 SiC 纳米线的接头形成包裹与保护作用，从而使接头部分具有更好的导电性、抗辐照性与导热性，提升了器件的稳定性与使用寿命。基于飞秒激光还原 GO 薄膜，实现 SiC 纳米线之间的电导通，可以进一步跨尺度制备 SiC 纳米线网络。该结构可以制备具有良好响应强度和较快响应速度的紫外光传感器，以及透明柔性导电薄膜等器件，为纳米线连接技术在跨尺度器件的广泛应用提供了新的思路。

致谢 本研究得到清华大学机械工程系邹贵生教授的大力支持和指导。

参 考 文 献

[1] Xiao M, Zheng S, Shen D Z, et al. Laser-induced joining of nanoscale materials: processing, properties, and applications[J]. Nano Today, 2020, 35: 100959.

[2] Chopra K L, Major S, Pandya D K, et al. Transparent conductors: a status review[J]. Thin Solid Films, 1983, 102(1): 1-46.

[3] Walsh A, Kehoe A B, Temple D J, et al. PbO_2: from semi-metal to transparent conducting oxide by defect chemistry control[J]. Chemical Communications, 2013, 49(5): 448-450.

[4] Wu J B, Agrawal M, Becerril H A, et al. Organic light-emitting diodes on solution-processed graphene transparent electrodes[J]. ACS Nano, 2010, 4(1): 43-48.

[5] Shen D Z, Xiao M, Zou G S, et al. Self-powered wearable electronics based on moisture enabled electricity generation[J]. Advanced Materials, 2018, 30(18): e1705925.

[6] Park D W, Kim B S, Park S, et al. Bipolar strain sensor based on an ultra-thin film of single-walled carbon nanotubes[J]. Journal of the Korean Physical Society, 2014, 64(3): 488-491.

[7] Kang M G, Kim M S, Kim J, et al. Organic solar cells using nanoimprinted transparent metal electrodes[J]. Advanced Materials, 2008, 20(23): 4408-4413.

[8] Rogers J A, Someya T, Huang Y G, et al. Materials and mechanics for stretchable electronics[J]. Science, 2010, 327(5973): 1603-1607.

[9] Lin L C, Liu L, Musselman K, et al. Plasmonic-radiation-enhanced metal oxide nanowire heterojunctions for controllable multilevel memory [J]. Advanced Functional Materials, 2016, 26(33): 5979-5986.

[10] Xing S L, Lin L C, Huo J P, et al. Plasmon-induced heterointerface thinning for Schottky barrier modification of core/shell SiC/SiO_2 nanowires [J]. ACS Applied Materials & Interfaces, 2019, 11(9): 9326-9332.

[11] Xiao Y, Shen D Z, Zou G S, et al. Self-powered, flexible and remote-controlled breath monitor based on TiO_2 nanowire networks [J]. Nanotechnology, 2019, 30(32): 325503.

[12] Song T B, Chen Y, Chung C H, et al. Nanoscale Joule heating and electromigration enhanced ripening of silver nanowire contacts[J]. ACS Nano, 2014, 8(3): 2804-2811.

[13] Chen C X, Yan L J, Kong E S W, et al. Ultrasonic nanowelding of carbon nanotubes to metal electrodes [J]. Nanotechnology, 2006, 17(9): 2192-2197.

[14] Zhang L Q, Tang Y S, Peng Q M, et al. Ceramic nanowelding[J]. Nature Communications, 2018, 9(1): 1-7.

[15] Garnett E C, Cai W S, Cha J J, et al. Self-limited plasmonic welding of silver nanowire junctions [J]. Nature Materials, 2012, 11(3): 241-249.

[16] Teng D, Zhao Y Z, Wang Y C, et al. Graphene plasmonic waveguide based on silicon-on-insulator structures [J]. Laser & Optoelectronics Progress, 2020, 58(3): 032301.
滕达, 赵永哲, 王云成, 等. 基于硅-绝缘体结构的石墨烯等离激元波导[J]. 激光与光电子学进展, 2020, 58(3): 032301.

[17] Liao J N, Wang X D, Zhou X W, et al. Femtosecond laser direct writing of copper microelectrodes [J]. Chinese Journal of Lasers, 2019, 46(10): 1002013.
廖嘉宁, 王欣达, 周兴汶, 等. 飞秒激光直写铜微电极研究[J]. 中国激光, 2019, 46(10): 1002013.

[18] Lin L C, Zou G S, Liu L, et al. Plasmonic engineering of metal-oxide nanowire heterojunctions in integrated nanowire rectification units[J]. Applied Physics Letters, 2016, 108(20): 203107.

[19] Xing S L, Lin L C, Zou G S, et al. Two-photon absorption induced nanowelding for assembling ZnO nanowires with enhanced photoelectrical properties [J]. Applied Physics Letters, 2019, 115(10): 103101.

[20] Teng D, Wang K, Li Z, et al. Graphene gap plasmonic waveguide for deep-subwavelength transmission of mid-infrared waves[J]. Acta Optica Sinica, 2020, 40(6): 0623002.
滕达, 王凯, 李哲, 等. 用于中红外波深度亚波长传输的石墨烯间隙等离激元波导[J]. 光学学报, 2020, 40(6): 0623002.

[21] Shown I, Hsu H C, Chang Y C, et al. Highly efficient visible light photocatalytic reduction of CO_2 to hydrocarbon fuels by Cu-nanoparticle decorated graphene oxide[J]. Nano Letters, 2014, 14(11): 6097-6103.

[22] Yeh T F, Chan F F, Hsieh C T, et al. Graphite oxide with different oxygenated levels for hydrogen and oxygen production from water under illumination: the band positions of graphite oxide[J]. The Journal of Physical Chemistry C, 2011, 115(45): 22587-22597.

[23] Reshanov S A, Emtsev K V, Speck F, et al. Effect of an intermediate graphite layer on the electronic properties of metal/SiC contacts[J]. Physica Status Solidi (b), 2008, 245(7): 1369-1377.

[24] Zhong H J. Studies on the contact properties of graphene and wide gap semiconductor materials[D]. Shenzhen: University of Chinese Academy of Sciences, 2012.
钟海舰. 石墨烯与宽禁带半导体材料的接触特性研究[D]. 深圳: 中国科学院大学, 2012.

[25] Gengler R Y N, Badali D S, Zhang D F, et al. Revealing the ultrafast process behind the photoreduction of graphene oxide [J]. Nature Communications, 2013, 4: 2560.

[26] Zou T T, Zhao B, Xin W, et al. High-speed femtosecond laser plasmonic lithography and reduction of graphene oxide for anisotropic photoresponse[J]. Light: Science & Applications, 2020, 9: 69.

[27] Kasischke M, Maragkaki S, Volz S, et al. Simultaneous nanopatterning and reduction of graphene oxide by femtosecond laser pulses [J]. Applied Surface Science, 2018, 445: 197-203.

[28] Han S, Hong S, Ham J, et al. Fast plasmonic laser nanowelding for a Cu-nanowire percolation network for flexible transparent conductors and stretchable electronics[J]. Advanced Materials, 2014, 26(33): 5808-5814.

Electrical Enhancement of SiC Nanowire Joints Based on Femtosecond Laser Reduction of GO

Huo Jinpeng[1], Xiao Yu[1], Sun Tianming[1,2], Xing Songling[1], Shen Daozhi[1], Lin Luchan[1,3], Liu Lei[1*]

[1] *State Key Laboratory of Tribology-Tsinghua University, Department of Mechanical Engineering, Tsinghua University, Beijing* 100084, *China*;

[2] *College of Materials Science and Engineering, Taiyuan University of Technology, Taiyuan, Shanxi* 030024, *China*;

[3] *Swiss Federal Laboratories for Materials Science and Technology, Zurich, Switzerland*

Abstract

Objective With the rapid development of information technology, aerospace technology, biotechnology and other fields, there are more demands for the miniaturization, integration, low power consumption and application of its equipment. Due to the unique small size effect, surface effect and quantum size effect, nanomaterials have a very broad application prospect in the new generation of semiconductor devices. As a bottom-up forming method of nanomaterials, welding and joining of nanoscale materials provide a technical mean for high-performance micro/nano devices and various cross-scale applications, such as memristors, field effect transistors, sensors and so on. Although the concept of nanowire bonding has been put forward very early, the theory of nanowire bonding has not been fully established, and the existing nanojoining methods made high demands on spatial accuracy of energy input and external environment. In view of this, we considered graphene oxide (GO) as the intermediate layer to join nanowires. In this paper, we introduce graphene oxide as an auxiliary conductive path at a fixed point in space, and use the reduction effect of femtosecond laser and the characteristics of local energy input to reduce graphene oxide locally. As a way of direct energy input, ultrafast laser can quickly adjust the energy input in space domain and time domain through optical lens and photoelectric shutter. The theoretical point contact joint was optimized as line contact and area contact, so as to improve the current level and performance. In addition, the protective effect of reduced graphene oxide (rGO) nanofilms on the structure was further studied, and a series of nanowire network device such as ultraviolet (UV) detectors and flexible transparent conductive films were prepared.

Methods SiC nanowire-GO film-SiC nanowire structure was prepared by dry transfer method (Fig. 1). The transfer process of a single nanomaterial is as follows: 10 μL of SiC nanowires suspension was placed on polydimethylsiloxane (PDMS) with a pipette gun. After evaporation of alcohol, SiC nanowires were moved to the designated position by using the nano transfer platform under the light microscope. The structure of SiC nanowire-GO film-SiC nanowire can be obtained by repeating the above steps. The reduction of GO films are achieved by femtosecond laser irradiation (50 fs pulse duration, 800 nm wavelength and 1 kHz frequency). The surface morphology and crystalline structure of SiC nanowire-GO film-SiC nanowire structures were obtained by scanning electron microscope (SEM, Zeiss Supra 55) and X-ray diffraction (XRD, Bruker D8). The electrical characterization of SiC nanowire-GO film-SiC nanowire structures was examined by a probe station (Keithley 2636B). The simulation of light field irradiation was carried out by multi-physical field finite element simulation software (COMSOL multiphysics 5.4). In the frequency domain module of wave optics, the wavelength of incident light was set to 800 nm, the intensity of incident electric field was set to 1, and the material parameters were inquired through related literature.

Results and Discussions After femtosecond laser irradiation, the current levels at both ends of the SiC nanowire-GO film-SiC nanowire structures are significantly improved (Fig. 3). The improvement of electrical properties of SiC nanowire-SiC nanowire-GO film structures is mainly due to the formation of intralayer conductive paths of rGO (Fig. 2), while the improvement of SiC nanowire-GO film-SiC nanowire structure is due to the formation of interlayer and intralayer conductive paths of rGO. After the rGO formed by laser reduction is in contact with SiC semiconductor, the Fermi energy levels of SiC and rGO will move simultaneously due to a small amount of carrier transport at the interface, and reach equilibrium. The contact barrier between rGO and SiC is significantly lowered (Fig. 5). The spatial electric field distribution shows that the electric field at the interface of graphene and

nanowires will be enhanced, which further promotes the two-photon absorption of GO for femtosecond laser, and improves the reduction efficiency (Fig. 6). For the ultraviolet sensor device constructed by SiC nanowire network, the photoelectric response characteristic before femtosecond laser irradiation is less than 10^{-5} A/W when it is irradiated by ultraviolet light with wavelength of 375 nm. After femtosecond laser irradiation, although the dark current of SiC nanowire network increased significantly, it showed a good response intensity and faster response speed to ultraviolet light. The responsivity of the optical sensor was about 0.11 A/W, which was improved by more than four orders of magnitude. Moreover, we used SiC nanowires and GO film to construct a transparent flexible conductive film on PDMS. After femtosecond laser scanning irradiation, the regional current of the conductive film was increased by more than five orders of magnitude (Fig. 7). This kind of flexible and transparent conductive film can be used in the fabrication of extensible flexible electrode or touch screen panel in the future.

Conclusions In this paper, the SiC nanowire-GO nanofilm-SiC nanowire structures were prepared by dry transfer method, then graphene oxide was reduced by femtosecond laser irradiation, which reduced the barrier between SiC and GO, and a wider carrier channel was formed through the way of intra layer and inter layer conduction, which significantly increased the current level of this structure. In addition, the obtained rGO nanofilms can wrap and protect the joints of SiC nanowires, which makes the joint have better radiation resistance and heat conduction, so as to improve the stability and service life of the device. Finally, the field effect transistor with low loss and high stability, UV sensor with good response and fast response, and transparent flexible conductive film were fabricated from SiC nanowire network with GO film by femtosecond irradiation.

Key words laser manufacture; femtosecond laser; silicon carbide nanowires; graphene oxide; micro/nano devices

OCIS codes 320.7090; 160.4236; 350.3390